PAPER Special Section of Papers Selected from ITC-CSCC'97

Structure of Delayless Subband Adaptive Filter Using Hadamard Transformation

Kiyoshi NISHIKAWA†, *Member*, Takuya YAMAUCHI†, *Student Member*, *and* Hitoshi KIYA†, *Member*

SUMMARY In this paper, we consider the selection of analysis filters used in the delayless subband adaptive digital filter (SBADF) and propose to use simple analysis filters to reduce the computational complexity. The coefficients of filters are determined using the components of the first order Hadamard matrix. Because coefficients of Hadamard matrix are either 1 or −1, we can analyze signals without multiplication. Moreover, the conditions for convergence of the proposed method is considered. It is shown by computer simulations that the proposed method can converge to the Wiener filter.

key words: *adaptive digital filter, delayless, Hadamard transform*

1. Introduction

In this paper, the selection of analysis filters used in the delayless subband adaptive digital filter (SBADF) [1] is considered. We propose to use the components of the first order Hadamard matrix as the coefficients of analysis filters to reduce computational complexity.

SBADF is a parallel adaptive system implemented by decomposing signals in the frequency domain using filter banks. The conventional structure of SBADF [2]–[5] is composed of analysis and synthesis banks to analyze and synthesize signals and a set of ADFs are driven in subbands at reduced clock rate. Using this structure, we can divide a high-order adaptation problem into lower order ones. This feature provides us a possibility to reduce computational complexity or to improve the convergence characteristics of adaptive algorithms or both. On the other hand, in some applications however, problems arise that filter banks generate transmission delay of the system and that aliasing components produced in analysis process generate bias to the optimal filter [1], [2]. These problems prevent SBADFs to achieve good adaptation characteristics.

In order to avoid these problems, Morgan and Thi proposed a new structure of SBADF. Delayless SBADF [1] realizes subband adaptation without generating transmission delay. Besides, they also showed that the structure has a possibility to eliminate the affection of aliasing components. In this structure, only analysis filters are used and, instead of synthesis bank, two kinds of ADFs are used, subband ADFs and a fullband one. After the coefficients of ADFs in subbands are updated, they are transformed into those of the fullband ADF. This transformation provides the above mentioned advantages, and the transformation is required to ensure the optimal filter of the fullband ADF will converge to the Weiner filter for the selected order. As the transformation from subband ADFs to the fullband one, [1] proposes to use DFT and IDFT. However, they do not clarify the relation between the transformation used and the optimal solution of the fullband filter. Moreover, no consideration on the convergence property nor on the selection of analysis filters used in delayless SBADF are given in [1].

In [6], [7], from theoretical considerations, Hirayama and Sakai showed that we cannot uniquely determine the coefficients of SBADFs from Wiener filter for the fullband one if DFT transformation is used in the delayless structure. In other words, the fullband ADF might not converge to the Weiner filter. As a transformation which promises the optimal solution would be consistent with the Wiener filter for the fullband ADF, they proposed a simpler transformation based on the Hadamard transform. However, the selection of analysis filters of delayless SBADF and conditions for convergence are not developed yet.

In this paper we consider the selection of analysis filters and propose to use simple filters as analysis filters used in the delayless SBADF. The coefficients of filters are determined using the components of the Hadamard matrix. Using the proposed method, amounts of computation can be reduced. Because each component of Hadamard matrix is either 1 or −1, we can analyze signals without multiplication. We also consider the conditions for convergence of the proposed method and show by computational simulations that the proposed method can converge to the Weiner solution.

This paper is organized as follows. In Sect. 2, we give a review of delayless SBADF [6], [7]. Section 3 considers the selection of analysis filters used in the delayless SBADF and the proposed method is described. In Sect. 4, we show the conditions for convergence of this method. To show the efficiency of the proposed method we examine computational simulations in Sect. 5.

Manuscript received September 30, 1997.
Manuscript revised December 23, 1997.

†The authors are with the Graduate School of Engineering, Tokyo Metropolitan University, Hachioji-shi, 192–0397 Japan.

2. Delayless Subband ADF

A structure of delayless SBADF with M-channel is shown in Fig. 1. In this figure, $x(n)$, $e(n)$ and $d(n)$ are the input, the error and the desired signals respectively. $\{H_i(z), i = 0, \ldots, M-1\}$ are analysis filters and D shows the decimation ratio. Note that, in the following, we use the notation n to indicate the time index at the clock rate of $x(n)$, and this means subband ADFs are updated at every D times.

$\{G_i(z), i = 0, \ldots, M-1\}$ are adaptive filters in each subband and $W(z)$ is the fullband ADF of this structure. The weight vectors of $W(z)$ and $G_i(z)$ are given as

$$\boldsymbol{w}(n) = [w_0(n), w_1(n), \ldots, w_{S-1}(n)]^T \quad (1)$$

$$\boldsymbol{g}_i(n) = [g_i(0), g_i(1), \ldots, g_i(N-1)]^T, \quad i = 0, \ldots, M-1 \quad (2)$$

where S is the length of $W(z)$, $N(= S/M)$ is the length of $G_i(z)$ and ^{T} denotes transpose operation. Using $H_i(z)$, both $x(n)$ and $e(n)$ are analyzed into subband signals and then they are used to update $G_i(z)$. We denote subband input vector and subband error signal in ith channel by $\boldsymbol{x}_i(n)$ and $e_i(n)$ respectively.

In each channel, $\boldsymbol{g}_i(n)$ are updated using the LMS type algorithm as

$$\boldsymbol{g}_i(n+1) = \boldsymbol{g}_i(n) + \mu_i \boldsymbol{x}_i(n) e_i(n), \quad i = 0, \ldots, M-1 \quad (3)$$

where μ_i is the step-size parameter in ith channel. After subband filters are updated according to (3), $\boldsymbol{g}_i(n)$ are transformed into $\boldsymbol{w}(n)$, the fullband ADF. In [6], [7], the following transformation is used to transform $g(n)$ into fullband weights $w(n)$;

$$w_k(n) = \frac{1}{2}\left[g_0\left(\left\lceil\frac{k}{2}\right\rceil\right) + (-1)^k g_1\left(\left\lceil\frac{k}{2}\right\rceil\right)\right] \quad (4)$$
$$k = 0, 1, \ldots, S-1,$$

in the two-channel case, where $\lceil x \rceil$ denotes the largest integer not exceeding x. In the z-domain, (4) is written as

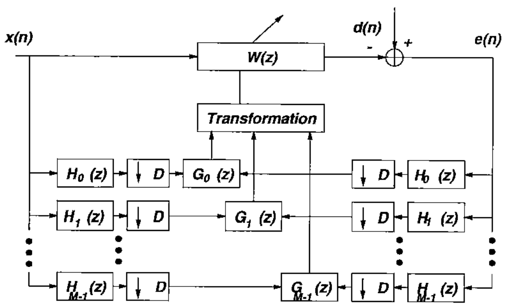

Fig. 1 Structure of delayless subband adaptive filters (M-channel).

$$W(z) = \frac{1}{2}[(1 + z^{-1})G_0(z^2) + (1 - z^{-1})G_1(z^2)]. \quad (5)$$

Note that (5) is identical to the Hadamard transform [6], [7].

We can extend this transformation into the M-channel case, where $M = 2^p$ and p is an integer greater than 1, by recursively applying (4). In this case, transformation is given as [6], [7]

$$\boldsymbol{w}_f(k) = \frac{1}{M}\boldsymbol{H}(p)\boldsymbol{w}_s(k) \quad (6a)$$

$$\boldsymbol{w}_f(k) = [w_{Mk}(n)\ w_{Mk+1}(n)\ \ldots\ w_{Mk+M-1}(n)]^T \quad (6b)$$

$$\begin{aligned}\boldsymbol{w}_s(k) = [&g_0(k) g_{M/2}(k) g_{M/4}(k) g_{3M/4}(k) g_{M/8}(k) \\ &g_{5M/8}(k) g_{3M/8}(k) g_{7M/8}(k) \ldots g_{M-2}(k) \\ &g_1(k) g_{M/2+1}(k) g_{M/4+1}(k) \ldots g_{M-1}(k)]^T,\end{aligned} \quad (6c)$$

where $k = 0, 1, \ldots, N-1$ and $\boldsymbol{H}(p)$ is the standard form of p-th Hadamard matrix [8].

3. Proposed Method

In this section the proposed method is described. As mentioned in the introduction, there is no consideration on the selection of analysis filter of the delayless structure shown in Fig. 1. However, the selection of analysis filters is an important task because it affects the performance of the structure of SBADF. For example, the computational burden increases as the lengths of analysis filters increase. Further, the design and realization of analysis filters become complex as the number of channel increases.

To implement delayless SBADF with less computational complexity, we propose to use coefficients of the first order Hadamard transform as the coefficients of analysis filters $H_i(z)$.

3.1 Case of Two-Channel

First we describe the case of two-channel or $M = 2$. In this case, we propose to determine $H_0(z)$ and $H_1(z)$ as

$$\begin{bmatrix} H_0(z) \\ H_1(z) \end{bmatrix} = \begin{bmatrix} 1 + z^{-1} \\ 1 - z^{-1} \end{bmatrix} = \begin{bmatrix} 1 & 1 \\ 1 & -1 \end{bmatrix}\begin{bmatrix} 1 \\ z^{-1} \end{bmatrix}. \quad (7)$$

Note that the length of each filter is $2(= M)$ as can be seen from (7). The matrix in the right-hand side of (7) is the first order Hadamard matrix, whose elements are either 1 or −1. This feature enables us to analyze $x(n)$ and $e(n)$ into subband signals with only addition or subtraction operations so that computational amounts required to analyze signals can be greatly reduced. Note that, in the proposed method, we use the Hadamard transformation both as the transformation from $g_i(n)$ into $w(n)$ and as analysis filters $H_i(z)$.

3.2 Case of M-Channel

Next we extend the proposed method to the case of M-channel, where M is a power of two. Structures of M-channel can be realized using the tree-structure. Figure 2 shows a possible structure of the 4-channel case. The structure of analysis filters shown in Fig. 2 can be implemented equivalently as the one shown in Fig. 3. In this case, the transfer function of an analysis filter $H_0'(z)$ is given by noble identity for multirate systems [9] as

$$\begin{aligned} H_0'(z) &= H_0(z)H_0(z^2) = (1+z^{-1})(1+z^{-2}) \\ &= 1+z^{-1}+z^{-2}+z^{-3}. \end{aligned} \tag{8}$$

Therefore, analysis filters $\{H_i'(z), i=0,1,2,3\}$ are written as

$$\begin{aligned} \begin{bmatrix} H_0'(z) \\ H_1'(z) \\ H_2'(z) \\ H_3'(z) \end{bmatrix} &= \begin{bmatrix} 1+z^{-1}+z^{-2}+z^{-3} \\ 1+z^{-1}-z^{-2}-z^{-3} \\ 1-z^{-1}+z^{-2}-z^{-3} \\ 1-z^{-1}-z^{-2}+z^{-3} \end{bmatrix} \\ &= \begin{bmatrix} 1 & 1 & 1 & 1 \\ 1 & 1 & -1 & -1 \\ 1 & -1 & 1 & -1 \\ 1 & -1 & -1 & 1 \end{bmatrix} \begin{bmatrix} 1 \\ z^{-1} \\ z^{-2} \\ z^{-3} \end{bmatrix} \\ &= \boldsymbol{H}'\boldsymbol{Z}, \end{aligned} \tag{9}$$

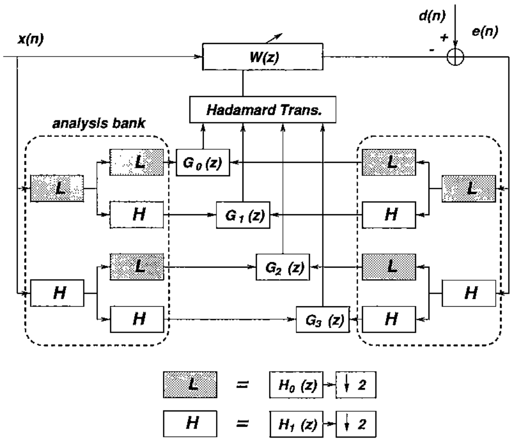

Fig. 2 Tree structure of proposed method in the case of $M=4$.

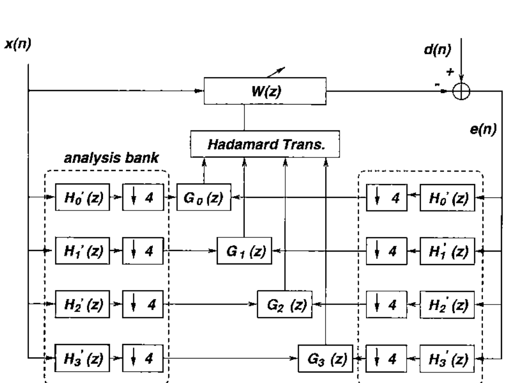

Fig. 3 Equivalent block diagram using noble identity in the case of $M=4$.

where $\boldsymbol{Z}$ is given as

$$\boldsymbol{Z} = [1, z^{-1}, z^{-2}, z^{-3}]^T. \tag{10}$$

The size of coefficient matrix of analysis filters is 4×4 in this case and will be $M \times M$ in the M-channel case. The characteristics that the components of $\boldsymbol{H}'$ are either 1 or -1 will be kept as in the two-channel case. We can analyze input signals into subband ones without multiplication.

3.3 Relation between $\boldsymbol{H}'$ and $\boldsymbol{H}(p)$

Here we describe the relation between $\boldsymbol{H}'$ and $\boldsymbol{H}(p)$, the standard form of Hadamard matrix, because $\boldsymbol{H}'$ in (9) is slightly different from $\boldsymbol{H}(p)$. Comparing $\boldsymbol{H}'$ with p-th order Hadamard matrix $\boldsymbol{H}(p)$, we can see that the elements of $\boldsymbol{H}'$ is expressed by permuting rows of $\boldsymbol{H}(p)$. The row vectors of $\boldsymbol{H}(p)$ are given as

$$\boldsymbol{H}(p) = \begin{bmatrix} \boldsymbol{h}_0 \\ \boldsymbol{h}_1 \\ \vdots \\ \boldsymbol{h}_{M-1} \end{bmatrix} \tag{11}$$

where

$$\begin{aligned} \boldsymbol{h}_i &= [h_{i,0} \ h_{i,1} \ \ldots \ h_{i,M-1}] \\ & \quad i = 0, 1, \ldots, M-1. \end{aligned} \tag{12}$$

By considering the order of $g_i(k)$ in (6c), we can determine how to permute row-vectors of $\boldsymbol{H}(p)$. As a result, $\boldsymbol{H}'$ is written as

$$\begin{aligned} \boldsymbol{H}' = [&\boldsymbol{h}_0^T \ \boldsymbol{h}_{M/2}^T \ \boldsymbol{h}_{M/4}^T \ \boldsymbol{h}_{3M/4}^T \ \boldsymbol{h}_{M/8}^T \ \cdots \ \boldsymbol{h}_{M-2}^T \\ &\boldsymbol{h}_1^T \ \boldsymbol{h}_{M/2+1}^T \ \boldsymbol{h}_{M/4+1}^T \ \boldsymbol{h}_{3M/4+1}^T \ \cdots \ \boldsymbol{h}_{M-1}^T]^T, \end{aligned} \tag{13}$$

using row vectors of $\boldsymbol{H}(p)$.

3.4 Computational Requirement

In this section, let us consider the computational requirement of the proposed method. In the case of M channel, where $M=2^p$ and p is an integer greater than 1, it is shown in Sect. 3.3 that the coefficients matrix of analysis filters is given by permuting row vectors of Hadamard matrix. This means that we can implement analysis bank using discrete Hadamard transform (DHT) algorithm [8], which resembles the FFT algorithm, and permutations.

Figure 4 shows a structure of analysis bank using DHT. Using this structure, the redundancy of computation can be eliminated. N-point DHT requires $N \log_2 N$ additions and subtractions and one multiplication. Because of delayless SBADF contains two analysis banks to analyze $x(n)$ and $e(n)$, computational requirement of the proposed method in the case of M-channel becomes

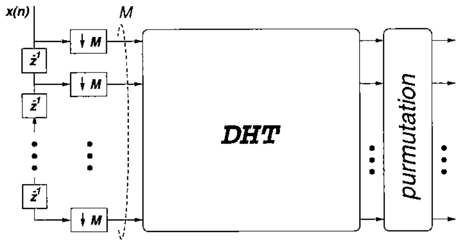

Fig. 4 Implementation of analysis bank using DHT.

$$\Omega_{a,prop} = 2\log_2 M \tag{14}$$

additions and subtractions at one clock rate of input signal $x(n)$, and two multiplications.

For a comparison, let us consider the delayless SBADF in [6], [7] and the conventional SBADF using analysis and synthesis banks [2]–[5].

When we implement delayless SBADF proposed in [6], [7] for the M-channel case, a tree structure can be used. In the tree structure, an intermediate operation will be repeated: an intermediate input signal is filtered and decimated by factor 2. When the length of analysis filters is L, this operation needs $L-1$ additions and L multiplications at the clock rate of an intermediate input. Therefore, in the M-channel case the computational requirement becomes

$$\Omega_{a,dless} = 2(L-1)\log_2 M \tag{15}$$

additions and

$$\Omega_{m,dless} = 2L\log_2 M \tag{16}$$

multiplications.

On the other hand, when DFT filter bank is used in the conventional structure [2]–[5], analysis and synthesis banks are implemented using one prototype filter, which is used as polyphase filters, and the DFT [9]. In the case of $M = 2^p$, FFT algorithm can be used to calculate DFT. For real input signal, an N-point FFT requires $(3N\log_2 N - 3N + 4)$ real additions and $(N\log_2 N - 5M + 4)$ real multiplications, where each addition can be implemented with two real additions and each complex multiplication can be implemented with three real multiplications and three real additions [10]. The conventional structure uses two analysis banks and one synthesis bank. Therefore, computational requirement of the conventional structure in the case of M-channel is

$$\Omega_{a,conv} = \frac{3(K + 3M\log_2 M - 3M + 4)}{M} \tag{17}$$

real additions and

$$\Omega_{m,conv} = \frac{3(K - M + 3M\log_2 M - 3M + 4)}{M} \tag{18}$$

real multiplications per input rate, where K is the length of the prototype filter.

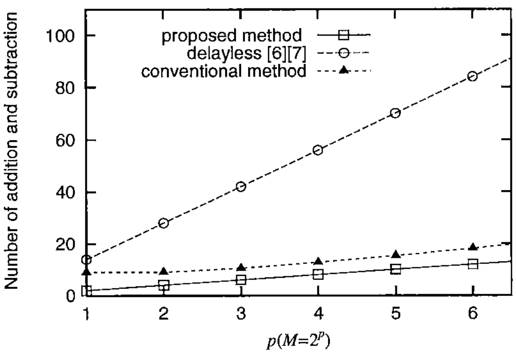

Fig. 5 Computational requirement for addition and subtraction. *delayless* uses 8taps analysis filters. *conventional method* uses $4M$taps prototype filters.

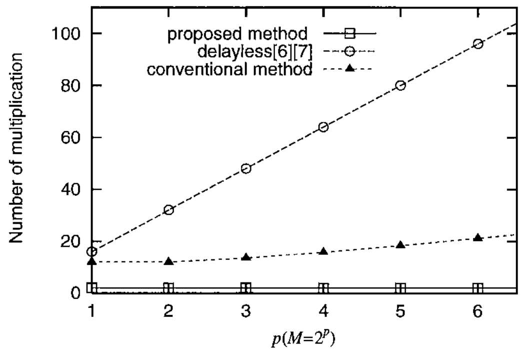

Fig. 6 Computational requirement for multiplication. *delayless* uses 8taps analysis filters. *conventional method* uses $4M$taps prototype filters.

Figures 5 and 6 show an example of the computational requirement described above. The lengths of analysis filters in the case of delayless SBADF in [6], [7] are 8. In the case of conventional structure the length of prototype filter K is set as $4M$. We can see from Fig. 5 and Fig. 6 computational complexity is reduced in the case of proposed method.

4. Condition for Convergence

In this section, we consider the condition for convergence of the proposed method and describe a method to determine the step-size parameter. [11] proposes a formula to determine step-size parameter to ensure the convergence of ADFs regardless of the employed analysis filter bank and characteristics of input signals. Here, we derive the condition under a restriction that the length of filter is equal to M. First, let us consider the case of two-channel and then, M-channel case will be considered.

4.1 Expression of Down- and Up-Sampling Using Matrices

We introduce an expression of down- and up-sampling using matrices in this section. When number of channel is 2, the matrix for expressing the decimation is given by

$$\boldsymbol{D}_N = [\boldsymbol{\phi}_{N,0}, \mathbf{o}_N, \boldsymbol{\phi}_{N,1}, \mathbf{o}_N, \ldots \boldsymbol{\phi}_{N,S-1}, \mathbf{o}_N] \quad (19)$$

where $\boldsymbol{\phi}_{N,k}$ and $\mathbf{o}_N$ are

$$\boldsymbol{\phi}_{N,k} = [\overbrace{0,\ldots,0}^{k}, 1, \overbrace{0,\ldots,0}^{N-1-k}]^T \quad (20a)$$

$$\mathbf{o}_N = [\overbrace{0\ 0\ \ldots\ 0}^{N}]^T \quad (20b)$$

and the size of $\boldsymbol{D}_N$ is $N \times S$.

For interpolation, we have 2 matrices defined as

$$\boldsymbol{U}_{N,0} = \begin{bmatrix} \boldsymbol{\phi}_{N,0}^T \\ \mathbf{o}_N^T \\ \boldsymbol{\phi}_{N,1}^T \\ \mathbf{o}_N^T \\ \vdots \\ \boldsymbol{\phi}_{N,S-1}^T \\ \mathbf{o}_N^T \end{bmatrix}, \boldsymbol{U}_{N,1} = \begin{bmatrix} \mathbf{o}_N^T \\ \boldsymbol{\phi}_{N,0}^T \\ \mathbf{o}_N^T \\ \boldsymbol{\phi}_{N,1}^T \\ \vdots \\ \mathbf{o}_N^T \\ \boldsymbol{\phi}_{N,S-1}^T \end{bmatrix} \quad (21)$$

and the size of $\boldsymbol{U}_{N,i}$ is $S \times N$. Using these matrices we can express (4) as

$$\boldsymbol{w}(n) = \frac{1}{2}[\boldsymbol{U}_{N,0}\{\boldsymbol{g}_0(n) + \boldsymbol{g}_1(n)\} + \boldsymbol{U}_{N,1}\{\boldsymbol{g}_0(n) - \boldsymbol{g}_1(n)\}]. \quad (22)$$

4.2 Derivation of the Update Formula of Weight-Error Vector

By substituting (3) into (22), we have

$$\begin{aligned}\boldsymbol{w}(n+2) &= \boldsymbol{w}(n+1) \\ &= \boldsymbol{w}(n) + \mu[\boldsymbol{U}_{N,0}\{\boldsymbol{\xi}_0(n) + \boldsymbol{\xi}_1(n)\} \\ &\quad + \boldsymbol{U}_{N,1}\{\boldsymbol{\xi}_0(n) - \boldsymbol{\xi}_1(n)\}] \end{aligned} \quad (23)$$

where

$$\boldsymbol{\xi}_0(n) = e_0(n)\boldsymbol{x}_0(n), \boldsymbol{\xi}_1(n) = e_1(n)\boldsymbol{x}_1(n). \quad (24)$$

Note that the relation $\boldsymbol{w}(n+2) = \boldsymbol{w}(n+1)$ in the case of $M = 2$ and that this paper uses a single step-size parameter μ as

$$\mu \triangleq \frac{1}{2}\mu_0 = \frac{1}{2}\mu_1. \quad (25)$$

For the following description, we define $\Delta\boldsymbol{w}(n)$ as

$$\Delta\boldsymbol{w}(n) = \mu[\boldsymbol{U}_{N,0}\{\boldsymbol{\xi}_0(n) + \boldsymbol{\xi}_1(n)\} + \boldsymbol{U}_{N,1}\{\boldsymbol{\xi}_0(n) - \boldsymbol{\xi}_1(n)\}], \quad (26)$$

and the weight-error vector $\boldsymbol{\epsilon}(n)$ as

$$\boldsymbol{\epsilon}(n) = \boldsymbol{w}_{opt} - \boldsymbol{w}(n) \quad (27)$$

in order to analyze the convergence characteristics, where $\boldsymbol{w}_{opt}$ is the optimal weight vector of fullband ADF.

Using these notations, subband error signal $e_i(n)$ can be expressed as

$$\begin{aligned} e_i(n) &= \sum_{j=0}^{1} h_i(j)e(n-j) \\ &= \sum_{j=0}^{1} h_i(j)\boldsymbol{x}^T(n-j)[\boldsymbol{w}_{opt} - \boldsymbol{w}(n-j)] \\ &= \sum_{j=0}^{1} h_i(j)\boldsymbol{x}^T(n-j)\boldsymbol{\epsilon}(n-j) \end{aligned} \quad (28)$$

where

$$\boldsymbol{x}(n) = [x(n), x(n-1), \ldots, x(n-S+1)]^T \quad (29)$$

and $h_i(j)$ denotes the (i,j)th element of $\boldsymbol{H}'$. By substituting (7), we finally have

$$e_0(n) = \boldsymbol{x}^T(n)\boldsymbol{\epsilon}(n) + \boldsymbol{x}^T(n-1)\boldsymbol{\epsilon}(n-1) \quad (30a)$$

$$e_1(n) = \boldsymbol{x}^T(n)\boldsymbol{\epsilon}(n) - \boldsymbol{x}^T(n-1)\boldsymbol{\epsilon}(n-1). \quad (30b)$$

Similarly, subband input signals are expressed as

$$\boldsymbol{x}_0(n) = \boldsymbol{D}_N[\boldsymbol{x}(n) + \boldsymbol{x}(n-1)] \quad (31a)$$

$$\boldsymbol{x}_1(n) = \boldsymbol{D}_N[\boldsymbol{x}(n) - \boldsymbol{x}(n-1)]. \quad (31b)$$

Let us consider expressing $\Delta\boldsymbol{w}(n)$ in terms of $\boldsymbol{\epsilon}(n)$ to develop the analysis method of the convergence characteristic which is similar to that of the LMS algorithm.

By noting the relation $\boldsymbol{\epsilon}(n) = \boldsymbol{\epsilon}(n-1)$ at even *n*, using (30b) and (31b), $\boldsymbol{\xi}_i(n)$ is expressed as

$$\begin{aligned}\boldsymbol{\xi}_0(n) = \boldsymbol{D}_N[&\boldsymbol{x}(n)\boldsymbol{x}^T(n) + \boldsymbol{x}(n-1)\boldsymbol{x}^T(n) \\ &+ \boldsymbol{x}(n)\boldsymbol{x}^T(n-1) + \boldsymbol{x}(n-1)\boldsymbol{x}^T(n-1)]\boldsymbol{\epsilon}(n)\end{aligned} \quad (32a)$$

$$\begin{aligned}\boldsymbol{\xi}_1(n) = \boldsymbol{D}_N[&\boldsymbol{x}(n)\boldsymbol{x}^T(n) - \boldsymbol{x}(n-1)\boldsymbol{x}^T(n) \\ &- \boldsymbol{x}(n)\boldsymbol{x}^T(n-1) + \boldsymbol{x}(n-1)\boldsymbol{x}^T(n-1)]\boldsymbol{\epsilon}(n).\end{aligned} \quad (32b)$$

Therefore, $\Delta\boldsymbol{w}(n)$ is rewritten as

$$\begin{aligned}&\Delta\boldsymbol{w}(n) \\ &= 2\mu\boldsymbol{U}_{N,0}\boldsymbol{D}_N[\boldsymbol{x}(n)\boldsymbol{x}^T(n) + \boldsymbol{x}(n-1)\boldsymbol{x}^T(n-1)]\boldsymbol{\epsilon}(n) \\ &+ 2\mu\boldsymbol{U}_{N,1}\boldsymbol{D}_N[\boldsymbol{x}(n-1)\boldsymbol{x}^T(n) + \boldsymbol{x}(n)\boldsymbol{x}^T(n-1)]\boldsymbol{\epsilon}(n).\end{aligned} \quad (33)$$

By introducing the notation

$$\boldsymbol{R}(j,k) = \boldsymbol{x}(n-j)\boldsymbol{x}^T(n-k), \quad (34)$$

we can express $\Delta\boldsymbol{w}(n)$ as a function of $\boldsymbol{\epsilon}(n)$:

$$\begin{aligned}\Delta\boldsymbol{w}(n) &= 2\mu\boldsymbol{U}_{N,0}\boldsymbol{D}_N[\boldsymbol{R}(0,0) + \boldsymbol{R}(1,1)]\boldsymbol{\epsilon}(n) \\ &\quad + 2\mu\boldsymbol{U}_{N,1}\boldsymbol{D}_N[\boldsymbol{R}(1,0) + \boldsymbol{R}(0,1)]\boldsymbol{\epsilon}(n) \\ &= \mu\boldsymbol{\Gamma}_0\boldsymbol{\epsilon}(n), \end{aligned} \quad (35)$$

where

$$\boldsymbol{\Gamma}_0 = 2\boldsymbol{U}_{N,0}\boldsymbol{D}_N[\boldsymbol{R}(0,0)+\boldsymbol{R}(1,1)] + 2\boldsymbol{U}_{N,1}\boldsymbol{D}_N[\boldsymbol{R}(1,0)+\boldsymbol{R}(0,1)]. \quad (36)$$

By substituting (27) into (23), we have

$$\begin{aligned} \boldsymbol{w}(n+2) &= \boldsymbol{w}(n) + \Delta\boldsymbol{w}(n) \\ \boldsymbol{w}_{opt} - \boldsymbol{\epsilon}(n+2) &= \boldsymbol{w}_{opt} - \boldsymbol{\epsilon}(n) + \Delta\boldsymbol{w}(n) \\ \boldsymbol{\epsilon}(n+2) &= \boldsymbol{\epsilon}(n) - \Delta\boldsymbol{w}(n). \end{aligned} \quad (37)$$

Finally, from (35), $\boldsymbol{\epsilon}(n+2)$ is written as

$$\boldsymbol{\epsilon}(n+2) = [\boldsymbol{I} - \mu\boldsymbol{\Gamma}_0]\boldsymbol{\epsilon}(n). \quad (38)$$

Note that this is a similar form of the weight error recursions of the LMS algorithm. In the following, the convergence condition is derived using this equation.

4.3 The Conditions for Convergence

For $\boldsymbol{w}(n)$ to converge, we require $\boldsymbol{\epsilon}(n+2)$ to satisfy

$$E[||\boldsymbol{\epsilon}(n+2)||^2] < E[||\boldsymbol{\epsilon}(n)||^2] \quad (39)$$

or equivalently

$$E[\boldsymbol{\epsilon}^T(n)\boldsymbol{\epsilon}(n)] - E[\boldsymbol{\epsilon}^T(n+2)\boldsymbol{\epsilon}(n+2)] > 0 \quad (40)$$

where $E[\cdot]$ is expectation operator. The condition of μ to ensure the relation (39) is expressed using the largest eigenvalue of $\boldsymbol{\Gamma}_0$ as

$$0 < \mu < \frac{2}{\lambda_{max}} \quad (41)$$

where λ_{max} is the largest eigenvalue of $\boldsymbol{\Gamma}_0$ [11]. This condition is valid provided all the eigenvalues of $\boldsymbol{\Gamma}_0$ are real and positive.

We can see from (34) and (36) that the first term of $\boldsymbol{\Gamma}_0$ relates the auto-correlation of $\boldsymbol{x}(n)$ and the second one relates its cross-correlation. In the following analysis, we use the independence assumption [12], which is widely used in the analyses of LMS-type algorithms. Under the assumption, $\boldsymbol{x}(n)$ and $\boldsymbol{x}(n-1)$ are assumed to be independent vectors so that we might neglect the second term of $\boldsymbol{\Gamma}_0$. Therefore, $\boldsymbol{\Gamma}_0$ is assumed to be consisted of only auto-correlation matrices, and hence, we assume the eigenvalues of $\boldsymbol{\Gamma}_0$ are real and positive. Then, the fullband filter $\boldsymbol{w}(n)$ converges if the step-size parameter μ is set as [11]

$$\mu = \frac{\alpha}{\mathrm{Tr}[\boldsymbol{\Gamma}_0]} = \frac{\alpha}{\alpha_0(n)+\alpha_1(n)}, \quad 0 < \alpha < 2 \quad (42)$$

where

$$\alpha_0(n) = \boldsymbol{x}_0^T(n)\boldsymbol{x}_0(n) + \boldsymbol{x}_1^T(n)\boldsymbol{x}_1(n) \quad (43a)$$
$$\alpha_1(n) = \boldsymbol{x}_0^T(n)\boldsymbol{x}_0(n-1) - \boldsymbol{x}_1^T(n)\boldsymbol{x}_1(n-1) \quad (43b)$$

and $\mathrm{Tr}[\cdot]$ denotes trace of matrix.

In the case of $M > 2$, we use the structure shown in Fig. 3. In this case, the lengths of analysis filters are equal to M, then the condition for $\boldsymbol{w}(n)$ to converge is given as a condition for the step-size parameter

$$\mu = \frac{\alpha}{\sum_{j=0}^{M-1}\sum_{i=0}^{M-1}\psi(i,j)\boldsymbol{x}_i^T(n)\boldsymbol{x}_i(n-j)} \quad (44)$$
$$0 < \alpha < 2$$

where $\psi(i,j)$ is an element of a matrix obtained by permuting the Hadamard matrix. $\psi(i,j)$ is consistent with $\boldsymbol{H}'$ shown in Sect. 3. Note that all the eigenvalue of $\boldsymbol{\Gamma}_0$ are assumed to be real and positive.

4.4 Approximation of (43)

To implement (42) and (44) is complicated because calculation of $\alpha_i(n)$ requires subband signals at different timing $(n-1)$. Let us consider to approximate (42).

In actual applications, we can say that the following relation can be assumed:

$$\alpha_0(n) \geqq \alpha_1(n) \quad (45)$$

as long as $\boldsymbol{x}(n)$ has the tapped delay-line characteristics [11]. Under this assumption, (42) can be approximated by

$$\begin{aligned}\mu &= \frac{\alpha}{2\alpha_0(n)} \\ &= \frac{\alpha}{2[\boldsymbol{x}_0^T(n)\boldsymbol{x}_0(n) + \boldsymbol{x}_1^T(n)\boldsymbol{x}_1(n)]}, 0 < \alpha < 2 \end{aligned} \quad (46)$$

This equation is simpler and easier to implement than (42). Similarly, in the case of M-channel, under this assumption, (44) can be approximated by

$$\mu = \frac{\alpha}{M\sum_{i=0}^{M-1}\psi(i,i)\boldsymbol{x}_i^T(n)\boldsymbol{x}_i(n)}, 0 < \alpha < 2 \quad (47)$$

5. Simulation

To show the efficiency of the proposed method described above, we examined the system identification problem by computer simulations. We show that the fullband filter $\boldsymbol{w}(n)$ will converge to the Wiener filter.

Conditions for simulations are as the following. The number of channel M was 2 or 4. Unknown system was given as an FIR filter of length 16. Number of tap of SBADF $G_i(z)$ was 8 in the case of $M = 2$ or 4 in the case of $M = 4$. Two input signals were used: A white Gaussian process and a colored process (AR(1) process with the AR parameter $\rho = 0.95$). The LMS algorithm was used for updating the weights of SBADF, and the step-size parameter μ was automatically determined by (46) and (47), and α was set as $\alpha = 1$ and 0.5. (6a) was used for transforming subband weights into fullband weights. As the reference of comparison we used the mean square error (MSE). All simulation results are the ensemble average of 20 independent processes.

For comparison, we show the convergence characteristics of the normalized LMS (NLMS) [12] with the step-size

$$\mu_{NLMS} = \frac{1}{\boldsymbol{x}(n)^T \boldsymbol{x}(n)}. \tag{48}$$

Also the conventional method [1] was simulated with the step-size

$$\mu_i = \frac{\beta}{\boldsymbol{x}_i(m)^T \boldsymbol{x}_i(m)}. \tag{49}$$

where two different values were used for β: $0.5, 1.0$ in the case of $M = 2$ and $0.1, 0.5$ in the case of $M = 4$. $\beta = 0.5$ $(M = 2)$ and 0.1 $(M = 4)$ seem to be the best values which were selected after some trials and $\beta = 1.0$ $(M = 2)$ and 0.5 $(M = 4)$ were selected for comparison. Figures 7 and 8 show the results of simulations for white Gaussian process and colored process respectively in the case of $M = 2$. Figures 9 and 10 show those in the case of $M = 4$. Note that horizontal and vertical axes of the figures show the clock rate of input signals and MSE respectively.

We can see from figures that the MSEs converge to about -300[dB] and this shows that the structure of delayless SBADF can eliminate the affection of the aliasing. However, it is also shown that the rate of convergence of delayless structure is much slower than NLMS.

We can confirm that, from the figures, the MSEs of the proposed method converges regardless of input process or the number of channels. On the other hand, the value for β of (49) must be re-selected to ensure the convergence as those conditions change. It is also shown that the conventional method can provide a faster rate of convergence if we can select the optimal value of β. However, there was no consideration on the range of β in the conventional researchers [1], [6], [7] so that it is hard to find the optimal value. The proposed method, in contrast, the step-size parameter can be automatically determined to ensure the convergence, although the rate of convergence is not the optimal. Improvement of the rate of convergence is considered to be our future work.

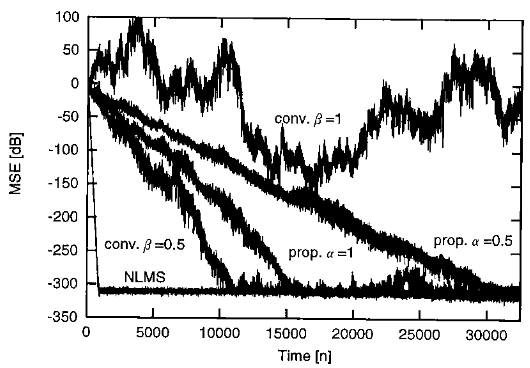

Fig. 7 MSE of proposed and conventional method in the case of $M = 2$. Input signal is a white Gaussian process. *prop.* is the result of using (46). The *conv.* are the results using (49) under $\beta = 1, 0.5$.

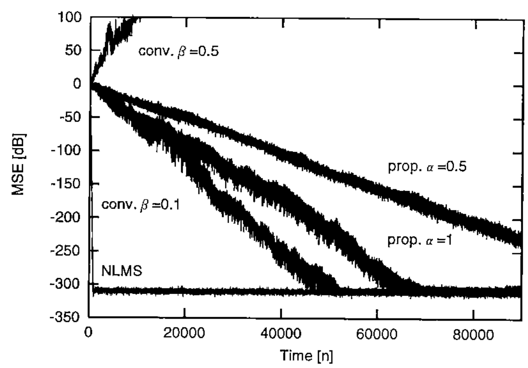

Fig. 9 MSE of proposed and conventional method in the case of $M = 4$. Input signals are white Gaussian process. *prop.* is the result of using (47) under $\alpha = 1, 0.5$. The *conv.* are the results using (49) under $\beta = 0.1, 0.5$.

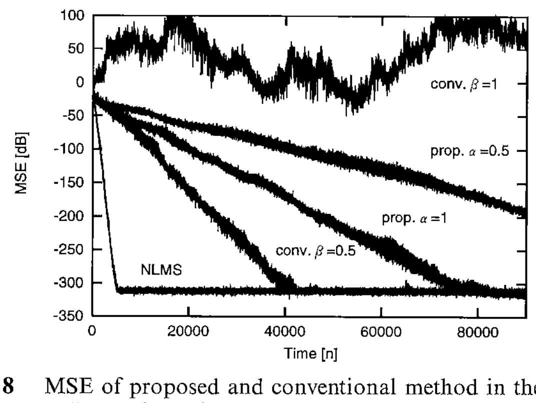

Fig. 8 MSE of proposed and conventional method in the case of $M = 2$. Input signal is a colored process. *prop.* is the result of using (46) under $\alpha = 1, 0, 5$. The *conv.* are the results using (49) under $\beta = 1, 0.5$.

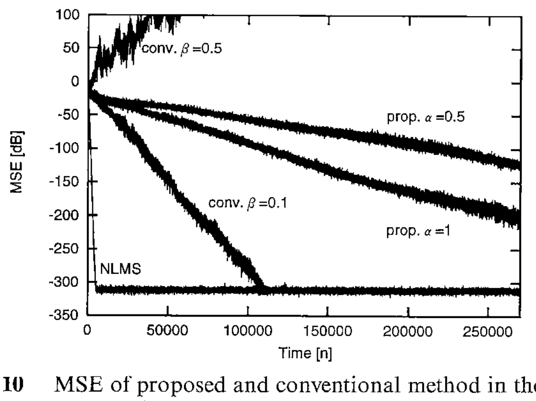

Fig. 10 MSE of proposed and conventional method in the case of $M = 4$. Input signal is a colored process. *prop.* is the result of using (47) under $\alpha = 1, 0, 5$. The *conv.* are the results using (49) under $\beta = 0.1, 0.5$.

6. Conclusion

The structure of delayless SBADF using simple analysis filters was proposed. We proposed to use the first order Hadamard matrix as the coefficients of analysis filters for the two-channel case. The structure of M-channel is realized using tree-structure or its equivalent structure. The advantage of the proposed method is that the analysis filters are simple, that is, their lengths are equal to the number of channels and their coefficients are either 1 or -1. Therefore no multiplication is needed for analyzing input signals into subband ones. Convergence of the proposed method was confirmed by computer simulations.

References

[1] D.R. Morgan and J.C. Thi, "A delayless subband adaptive filter architecture," IEEE Trans. Acoust., Speech & Signal Process, vol.43, pp.1819–1830, Aug. 1995.
[2] A. Gilloire and M. Vetterli, "Adaptive filtering in subbands with critical sampling: Analysis, experiments and application to acoustic echo cancellation, " IEEE Trans. Acoust., Speech & Signal Process., vol.40, pp.1862–1875, Aug. 1992.
[3] F. Amano, P. Meana, A. de Luca, and G. Duchen, "A multirate acoustic echo canceler structure, " IEEE Trans. Commun., vol.43, pp.2172–2176, July 1995.
[4] Y. Yamada, H. Ochi, and H. Kiya, "A subband adaptive filter allowing maximally decimation," IEEE J. Select. Area Commun., vol.12, pp.1548–1552, Dec. 1994.
[5] K. Ashihara, K. Nishikawa, and H. Kiya, "Improvement of convergence speed for subband adaptive digital filter using the multirate repeating method," Proc. IEEE ICASSP'95, Detroit, Michigan, U.S.A, pp.989–992, May 1995.
[6] N. Hirayama and H. Sakai, "Analysis of a delayless subband adaptive filter," Proc. 11th DSP Symposium, Tottori, Japan, pp.A5-2-1–A5-2-4, Nov. 1996.
[7] N. Hirayama and H. Sakai, "Analysis of a delayless subband adaptive filter," Proc. IEEE ICASSP'97, Munich, Germamy, pp.2329–2332, April 1997.
[8] A.K. Jain, "Fundamentals of Digital Image Processing," Prentice Hall, Englewood Chiffs, 1989.
[9] P.P. Vaidyanthan, "Multirate Systems and Filter Banks," Prentice Hall, 1993.
[10] H.V. Sorensen, D.L. Jones, M.T. Heideman, and C.S. Burrus, "Real-valued fast fourier transform algorithms," IEEE Trans. Acoust., Speech & Signal Process., vol.ASSP-35, pp.849–863, June 1987.
[11] K. Nishikawa and H. Kiya, "Conditions for convergence of a delayless subband adaptive filter and its efficient implementation," IEICE Technical Report, DSP97-42, June 1997.
[12] S. Hayiin, "Adaptive Filter Theory," Upper Saddle River, NJ 07458, Prentice Hall, 1996.

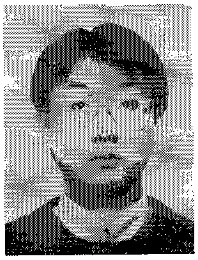

Kiyoshi Nishikawa was born in Tokyo, Japan, on December 12, 1966. He received the B.E., the M.E., and the D.E. degrees in electrical engineering from Tokyo Metropolitan University in 1990, 1992 and 1996, respectively. From 1992 to 1993, he was at the Computer Systems Laboratory, Nippon Steel Corp. as a researcher. Since 1993, he has been with Tokyo Metropolitan University as an Assistant Professor. His search interest includes the adaptive signal processing. He is a member of IEEE SP, CAS, IT, and Computer Society.

Takuya Yamauchi was born in Tokyo, Japan, on December 25, 1972. He received the B.E. degrees in electronics and information engineering from Tokyo Metropolitan University in 1996. He is currently a candidate for the M.E. degree at Tokyo Metropolitan University. His research interests are in adaptive signal processing.

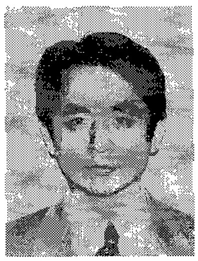

Hitoshi Kiya was born in Yamagata, Japan, on November 16, 1957. He received the B.E. and M.E. degrees in electrical engineering from Nagaoka University of Technology, Niigata, Japan, and the D.E. degree in electrical engineering from Tokyo Metropolitan University, Tokyo, Japan, in 1980, 1982 and 1987, respectively. In 1982, he joined Tokyo Metropolitan University, where he is currently an Associate Professor of Electrical Engineering, Graduate School of Engineering. He was a visiting researcher of the University of Sydney in Australia from Oct. 1995 to March 1996. His research interests are in digital signal processing, multirate systems, adaptive filtering, image processing, and efficient algorithms for VLSI implementation. He is now serving as an Associate Editor of the IEEE Trans. on Signal Processing. Dr. Kiya is a Member of IEEE, the Image Electronics Engineers of Japan and the Institute of Image Information and Television Engineers of Japan.